Sensitivity of Kinetic Ballooning Mode Instability to Tokamak Equilibrium Implementations

H. S. Xie,[1] Y. Xiao,[1,*] I. Holod,[2] Z. Lin,[2,3] and E. A. Belli[4]

[1] *Institute for Fusion Theory and Simulation, Department of Physics, Zhejiang University, Hangzhou, 310027, People's Republic of China*

[2] *Department of Physics and Astronomy, University of California, Irvine, California 92697, USA*

[3] *Fusion Simulation Center, Peking University, Beijing 100871, China*

[4] *General Atomics, P.O. Box 85608, San Diego, California 92186-5608, USA*

(Dated: March 26, 2015)

Global first-principle study of kinetic ballooning mode (KBM) is crucial to understand the tokamak edge physics in high-confinement mode (H-mode). Contrast to ion temperature gradient mode and trapped electron mode, KBM is found to be very sensitive to the equilibrium implementations in gyrokinetic codes. In this brief communication, we show that, a second order difference for magnetic equilibrium, or switch between the local and global profile implementations will bring a factor of two or more difference in real frequency and growth rate. This suggests that an accurate global equilibrium should be required for gyrokinetic simulation to verify codes and validate H-mode experiments with KBM. [2015-03-26 17:10 rev]

Ballooning mode[1] is an electromagnetic instability driven mainly by pressure gradient, and is considered to be one of the most important instabilities in the high-confinement mode (H-mode) stage of tokamaks. The H-mode is important for tokamaks since it can improve the plasmas confinement to make fusion economically more feasible. The ideal peeling-ballooning mode and kinetic ballooning mode are invoked to predict the formation of the H-mode pedestal[2]. The linear and nonlinear physics of the peeling-ballooning modes have been recently studied intensively by fluid codes, such as the eigenvalue code ELITE[3] and initial value code BOUT++[4], which have helped explain several important aspects (e.g., mode numbers) of the H-mode experiments (cf. [5]). However, the fluid models lack many important kinetic physics contents, such as the wave-particle resonance and finite Larmor radius effect, which may play a critical role in the formation of the H-mode pedesdal. A complete understanding of the electromagnetic instabilities in the tokamak edge is still in progress. Especially, first principle electromagnetic kinetic simulations have not been well verified after around one decade of efforts.

For the electrostatic tokamak plasmas, the equilibrium magnetic geometry is critical for quantitative study of the nonlinear physics[6–8]. It is found that ignoring the difference of the poloidal angle between the torus coordinates (r, θ_0, ζ_0) and flux coordinates (r_f, θ_f, ζ_f) could lead to significant differences in the turbulent transport simulated by various gyrokinetic codes[6, 7]. For the finite-beta plasmas, the electromagnetic effect may dominate and the implementation of magnetic equilibrium is found by global gyrokinetic simulation code GTC[11, 12] to be important for the linear physics. The semi-analytical global Shafranov equilibrium to second order is implemented[9, 10] in the GTC code to study the magnetic equilibrium effects for the electromagnetic KBM. It is found that a slight difference in the equilibrium can cause a large difference in the linear frequency and growth rate, let alone the nonlinear physics. The local and global profiles also provide rather different linear frequencies and growth rates.

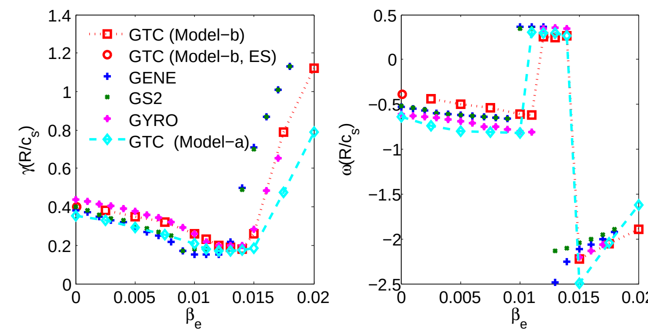

FIG. 1: Scanning β_e to benchmark GTC with other gyrokinetic codes GYRO, GENE and GS2 for different equilibrium field models. The transition from ITG to TEM, and to KBM is clear shown with β_e increasing. The equilibrium implementations do not affect ITG and TEM too much, but affect the KBM branch largely. Data are partly taken from Refs.[15–18]. ES means electrostatic simulation; The simulation codes except GTC are using Model-a equilibrium by default.

We consider a low β model equilibrium with $\beta \sim \epsilon^2$, where $\epsilon = r/R_0 \ll 1$ is the inverse aspect ratio. Under the boundary condition given by a circular conducting wall, the equilibrium flux surfaces are concentric circles to lowest order. To the second order, the flux surfaces are shifted circles, which can be defined in terms of the usual cylindrical coordinates (R, ϕ_c, Z) by the following

*Email: yxiao@zju.edu.cn

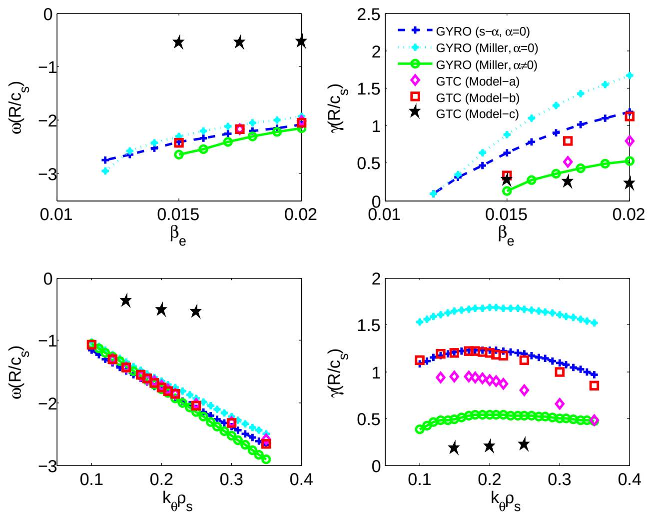

FIG. 2: GTC vs. GYRO for different equilibrium implementations. GYRO (s-α, $\alpha = 0$) is Model-a; GYRO (Miller, $\alpha = 0$) is Model-b; GYRO (Miller, $\alpha \neq 0$) is Model-c.

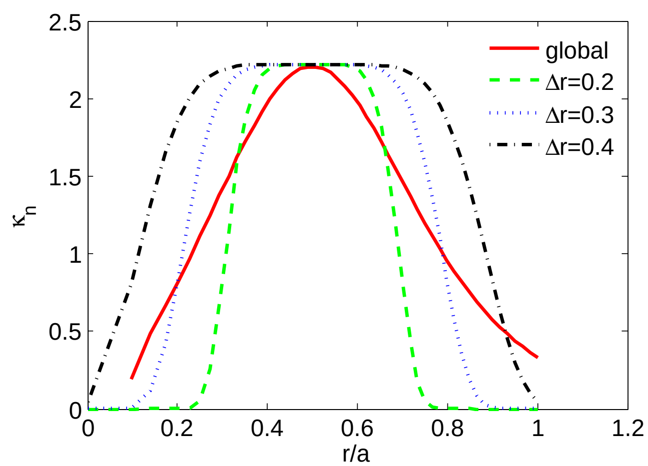

FIG. 3: Local and global profiles of κ_n used in GTC.

equations:

$$R = R_0 + r_s \cos\theta_s - \Delta(r_s), \quad (1a)$$
$$\phi_c = -\zeta_s, \quad (1b)$$
$$Z = r_s \sin\theta_s, \quad (1c)$$

where R_0 is the major radius and the Shafranov shift $\Delta(0) = 0$ (note: some authors use $\Delta|_{r_s=a} = 0$ but what really matters is the derivative of the Shafranov shift, where a is the minor radius). The relations between Boozer flux coordinates (r_f, θ_f, ζ_f) and geometry coordinates (r_s, θ_s, ζ_s) are $r = r_s$, $\zeta_f = \zeta_s$ and $\theta_f = \theta_s - (\epsilon + \Delta')\sin\theta_s$[13], with Δ' being the radial derivative of the Shafranov shift $\Delta(r) = \int_0^r \frac{q^2 dr}{r^3 R_0} \int_0^r \left[\frac{r^2}{q^2} - 2\frac{R_0^2}{B_0^2} r p'\right] r dr$[14], where q is the safety factor, B_0 is the on-axis magnetic field and p is the normalized pressure. In the gyrokinetic community, three types of so called s-α models are generally used, with Model-a: lowest order approximation $\theta = \theta_s$, Model-b: first order approximation without the Shafranov shift, $\Delta = 0$ and $\theta = \theta_s - \epsilon \sin\theta_s$, and Model-c: $\Delta \neq 0$ and $\theta = \theta_s - (\epsilon + \Delta')\sin\theta_s$.

Fig.1 shows the β_e scanning for the linear frequency and growth rate and compare the GTC results with those from other gyrokinetic codes GYRO, GENE and GS2, where the Cyclone base case parameters[19] are employed, i.e., $s = 0.78$, $q = 1.4$, $\kappa_T = R_0/L_T = 6.9$, $\kappa_n = R_0/L_n = 2.2$ and $T_i = T_e$, where $L_n = -d\ln n/dr$ and $L_T = -d\ln T/dr$. The transition from ITG to TEM and to KBM is clearly shown with β_e increasing. The GTC (Model-b) electromagnetic[12, 16] simulation at $\beta_e \to 0$ limit can recover the GTC (Model-b, ES) electrostatic[11] result, which confirms that the GTC electromagnetic model should be correct. The equilibrium implemented in other gyrokinetic codes is generally the above Model-a by default. In the GTC code, both Model-a and Model-b are implemented. As can been seen in Fig.1, the equilibrium implementation does not affect ITG, TEM and their transition much, but it affects the linear growth rate of KBM a lot. The GTC code gives real frequency for the KBM branch similar to other gyrokinetic codes, but a smaller growth rate, e.g., for the case with $\beta_e = 1.75\%$ and Model-a, $\gamma^{\mathrm{GYRO}} \simeq 1.5\gamma^{\mathrm{GTC}}$. We note that this difference could come from the difference of the equilibrium profiles, as is shown in the latter part of this paper. That is, other gyrokinetic codes like GYRO use local flux-tube equilibrium, whereas the GTC code uses a global equilibrium. A linear electromagnetic gyrokinetic study has been carried out for the DIII-D H-mode pedestal[20], which shows that the frequency and growth rate can have 50% deviation among several gyrokinetic codes with local equilibrium settings. We also note that the gyrokinetic code GEM with the flux-tube equilibrium shows good agreement with the aforementioned gyrokinetic codes such as GYRO for the ITG and TEM instabilities[22].

To further identify the effect of the equilibrium implementation, Fig.2 shows a more detailed scanning of the β_e and $k_\theta \rho_i$ for the KBM branch. We find a large discrepancy in both frequency and growth rate if the Shafranov shift is considered in the GTC's KBM simulation. Both ω_r and γ become much smaller with the Shafranov shift included. We have also compared the Shafranov shift effect on the ITG instability. In the GTC simulation, the differences of ω and γ between the equilibriums with and without Shafranov shift are less than 5%[10] and thus the shift effect is negligibly small. A study by GEM[21] predicts a dominant high frequency electromagnetic mode whose frequency has not been found in experiments. It is possible that the disagreement is from the local Miller equilibrium used in GEM, which would predict a much higher frequency for KBM. These findings suggest that an accurate global instead of local equilibrium model would be crucial to validate experiments with the gyrokinetic simulation.

To identify that the local equilibrium may not be suit-

TABLE I: Influence of the radial width of the local profiles to KBM and ITG.

ω	$\Delta r = 0.4$	$\Delta r = 0.3$	$\Delta r = 0.2$	global
KBM	1.67+1.09i	1.77+1.02i	1.90+0.93i	2.06+0.51i
ITG	0.47+0.16i	0.47+0.15i	0.48+0.14i	0.49+0.15i

able for validating experiments with KBM, we compare the results from different local and global equilibriums using the GTC code. In Figs.1&2, the following global profile for GTC is used: $q = 0.82 + 1.1(\psi/\psi_w) + 1.0(\psi/\psi_w)^2$, $n_i = n_e = 1.0 + 0.205\{\tanh[(0.3-(\psi/\psi_w))/0.4] - 1.0\}$ and $t_i = t_e = 1.0 + 0.415\{\tanh[(0.18-(\psi/\psi_w))/0.4] - 1.0\}$, where ψ is the poloidal flux and $\psi_w = \psi(r = a) = 0.0375 B_0 R_0^2$, which gives $a/R_0 = 0.36$ and the local parameters in $r = 0.5a$ (where is also the peaking gradient position for density and temperature) as the Cyclone based case. To model the local equilibrium profile, we use the following gradients to calculate the density and temperature profiles: $\kappa_n = 2.22e^{-[\frac{(r/a-0.5)}{\Delta r}]^6}$ and $\kappa_T = 6.92e^{-[\frac{(r/a-0.5)}{\Delta r}]^6}$, where Δr determine the radial width of the local profile. Fig.3 shows the κ_n used in GTC to model local equilibriums. In the electrostatic simulation for ITG and TEM, the linear frequency and growth rate are not sensitive to Δr. Table I shows the electromagnetic simulation results for ITG and KBM with different local profile widths Δr, which are compared with global profile. We see that the frequency and growth rate for ITG change little for different equilibrium implementations. However, the frequency and growth rate for KBM are very sensitive to the equilibrium implementation. To ensure that this difference comes from the equilibrium, the adiabatic electron and Model-a equilibrium are used in the simulation to exclude other factors. The only difference between the ITG and KBM is the β_e, i.e., $\beta_e^{\mathrm{ITG}} = 0.25\%$ and $\beta_e^{\mathrm{KBM}} = 1.75\%$. The results confirm that the KBM is very sensitive to the equilibrium and global profile. In addition, this suggests that an accurate global equilibrium should be required for gyrokinetic simulation to verify codes and validate H-mode experiments with KBM.

HSX would like to thank X. Q. Xu for useful discussions and J. Candy for information on the s-α model. The work is supported by the National Magnetic Confinement Fusion Science Program under Grant No. 2015GB110000, 2013GB111000, China NSFC under Grant No. 91130031, the Recruitment Program of Global Youth Experts, and US DOE SciDac GSEP centers.

[1] J. W. Connor, R. J. Hastie and J. B. Taylor, Phys. Rev. Lett., , **40**, 396 (1978).
[2] P. Snyder, R. Groebner, J. Hughes, T. Osborne, M. Beurskens, A. Leonard, H. Wilson and X. Xu, Nuclear Fusion, **51**, 103016 (2011).
[3] H. R. Wilson, P. B. Snyder, G. T. A. Huysmans and R. L. Miller, Phys. Plasmas, **9**, 1277 (2002).
[4] B. Dudson, M. Umansky, X. Xu, P. Snyder and H. Wilson, Computer Physics Communications, **180**, 1467 (2009).
[5] Z. X. Liu, X. Q. Xu, X. Gao, T. Y. Xia, I. Joseph, W. H. Meyer, S. C. Liu, G. S. Xu, L. M. Shao, S. Y. Ding, G. Q. Li, and J. G. Li, Phys. Plasmas, **21**, 090705 (2014).
[6] X. Lapillonne, S. Brunner, T. Dannert, S. Jolliet, A. Marinoni, L. Villard, T. Gorler, F. Jenko and F. Merz, Phys. Plasmas, **16**, 032308 (2009).
[7] Z. Lin, S. Ethier, T. S. Hahm and W. M. Tang, Plasma Sci. Technol., **14**, 1125 (2012).
[8] Y. Xiao and P. J. Catto, Phys. Plasmas, **13**, 082307 (2006).
[9] Y. Xiao, I. Holod, Z. Wang, Z. Lin and T. Zhang, Phys. Plasmas, **22**, 022516 (2015).
[10] H. S. Xie, Shifted Circular Tokamak Equilibrium with Application Examples, unpublished notes (`http://ifts.zju.edu.cn/student/hsxie/codes/shafeq/`), 2014.
[11] Z. Lin and T. S. Hahm, Phys. Plasmas, **11**, 1099 (2004).
[12] I. Holod, W. L. Zhang, Y. Xiao and Z. Lin, Phys. Plasmas, **16**, 16, 122307 (2009).
[13] J. D. Meiss and R. D. Hazeltine, Phys. Fluids B, **2**, 2563 (1990).
[14] R. B. White, *The Theory of Toroidally Confined Plasmas* (World Scientific Imperial College Press, 2001).
[15] E. A. Belli and J. Candy, Phys. Plasmas **17**, 112314 (2010).
[16] I. Holod and Z. Lin, Phys. Plasmas **20**, 032309 (2013).
[17] J. Candy, Phys. Plasmas **12**, 072307 (2005).
[18] M. J. Pueschel, M. Kammerer, and F. Jenko, Phys. Plasmas **15**, 102310 (2008).
[19] A. M. Dimits, G. Bateman, M. A. Beer, B. I. Cohen, W. Dorland et al., Phys. Plasmas, **7**, 969 (2000).
[20] E. Wang, X. Xu, J. Candy, R. Groebner, P. Snyder, Y. Chen, S. Parker, W. Wan, G. Lu and J. Dong, Nuclear Fusion, **52**, 103015 (2012).
[21] W. Wan, S. E. Parker, Y. Chen, R. J. Groebner, Z. Yan, A. Y. Pankin and S. E. Kruger, Phys. Plasmas, **20**, 055902 (2013).
[22] Y. Chen, S. E. Parker, W. Wan and R. Bravenec, Phys. Plasmas, **20**, 092511 (2013).
[23] Y. Chen, private communications, 2014.